

Multi-wavelength observations of post flare loops in two long duration solar flares

L.K. Harra-Murnion¹, B. Schmieder^{2,3}, L. van Driel-Gesztelyi^{2,4}, J. Sato⁵, S.P. Plunkett⁶, P. Rudawy⁷, B. Rompolt⁷, M. Akioka⁸, T. Sakao⁵, and K. Ichimoto⁵

¹ Mullard Space Science Laboratory, University College London, Holmbury St. Mary, Dorking, Surrey RH5 6NT, UK

² DASOP, Observatoire de Paris, F-92195 Meudon Principal Cedex, France

³ University of Oslo, P.O. Box 1029, Blindern, N-0315 Oslo, Norway

⁴ Konkoly Observatory, 1525 Budapest, P.O. 67, Hungary

⁵ National Astronomical Observatory, Mitaka, Tokyo 181, Japan

⁶ Universities Space Research Association, Naval Research Laboratory, Washington, DC 20375, USA

⁷ Astronomical Institute of Wrocław University, ul. Kopernika 11, PL-51622 Wrocław, Poland

⁸ Hiraio Solar Terrestrial Research Center, Communications Research Laboratory, Isozaki, Nakaminato-shi, 311-12 Ibaraki, Japan

Received 9 April 1998 / Accepted 2 July 1998

Abstract. We have analysed two Long Duration solar Events (LDEs) which produced large systems of Post Flare Loops (PFLs) and which have been observed by Yohkoh and ground-based observatories. Using the Maximum Entropy Method (MEM) image synthesis technique with new modulation patterns we were able to make hard X-ray (HXR) images of the post flare loops recorded in the L Channel (13.9–22.7 keV) of the Yohkoh Hard X-ray Telescope. We obtained co-aligned 2-D maps in $H\alpha$ (10^4 K), in soft X-rays (5×10^6 K) and in hard X-rays (20×10^6 K). We conclude that the soft X-ray (SXR) loops lie higher than the $H\alpha$ loops and the former are overlaid by HXR emission. This is suggestive of the magnetic reconnection process. However some details are not consistent with the standard models. Firstly the separation between the HXR source and the SXR loop increases with time, with the HXR source being approximately a factor of five larger than the equivalent source in impulsive flares. Secondly the cooling times deduced from observations are longer than the theoretically expected ones and the discrepancy increases with time. We review the current models in view of these results.

Key words: Sun: flares – Sun: X-rays, gamma rays

1. Introduction

Long Duration Events (LDEs) are generally associated with large well developed systems of loops called post-flare loops which are observed at different temperatures ranging from 10^4 to more than 10^6 K. These post-flare loops expand, lasting up to 10 hours (e.g. Bruzek 1964). The velocity of ascent of these loops decreases with time from 10–20 kms^{-1} to less than 1 kms^{-1} (e.g. Pneuman 1981, Bray et al. 1991 and references therein). This process of expansion is believed to be due to

ongoing magnetic reconnection (e.g. Kopp & Pneuman 1976). The newly formed hot loops cool down to appear eventually as $H\alpha$ loops. Some developments of theoretical models taking into account the evaporation process or siphon mechanisms can explain the long duration of these phenomena (Cargill and Priest 1983, Forbes and Malherbe 1986, Forbes and Acton 1996). Several authors including Moore et al. (1980) and MacCombie and Rust (1979), conclude that the Kopp and Pneuman model fits well with the majority of their observations.

Schmieder et al. (1995, 1996) and van Driel-Gesztelyi et al. (1997a) have recently observed cool $H\alpha$ loops of an LDE using data from several ground based instruments and hot loops (X-rays) with the Yohkoh spacecraft. They found that the cool loops lie tangentially below the hot loops and rise with a velocity of $\approx 1 \text{ kms}^{-1}$ upwards. They also observed a triangle of hot plasma at the top of the hot loops, which is indicative of a reconnection process (e.g. Forbes and Malherbe 1986).

Yohkoh observations have provided evidence that magnetic reconnection at a neutral sheet located at the looptop may be responsible for the energy release in some flares (e.g. Tsuneta et al. 1992, Masuda et al. 1994, Tsuneta 1996). A detailed study by Tsuneta et al. 1992 showed the following characteristics of an LDE: the looptop region has a cusp-like structure, the outer loops have a higher temperature in the decay phase and the apparent height of the loop and the separation of the footpoints increase with time.

Švestka et al. (1987b) studied the flare of 6 November 1980 which was observed by the HXIS and FCS instruments on board the Solar Maximum Mission (SMM) permitting observations of the loops in five different temperature regions from $H\alpha$ to Fe XXV (HXIS). The height of the loops was found to increase with successively higher temperatures. They emphasised that the time for the $H\alpha$ loops to appear at the same height as the X-ray loops was more than one hour whereas the cooling times derived from the measurements of temperature and density pre-

Send offprint requests to: L.K. Harra-Murnion

dict only two minutes. This discrepancy increased with time. From these results they concluded that the newly formed hot loops must shrink to lower heights before they are seen in $H\alpha$ due to an enhancement in loop density from evaporated material – the gravitational forces will cause the loops to collapse. Švestka (1996) also discusses the discovery of two separate structures which develop following the flare 21–22 May 1980 – the standard post flare loop system and a much higher scale structure which was visible in > 3.5 keV for more than 10 hours and was named post-flare giant arch. The giant arches have constant speed whereas the post-flare loop system normally have decreasing speed. The giant arches have also been observed by Yokoh. Švestka's interpretation is that the post-flare loop systems start with the Kopp and Pneuman process and in later stages the loops can be heated continuously.

Although there has been much support for the reconnection model with various modifications, there are a number of papers which disagree with these conclusions. Seely & Feldman (1984) use CaXIX spectra from the Bragg Crystal Spectrometer SOLFLEX on the U.S. Air Force P78-1 spacecraft. They have determined that the CaXIX emission region rises with velocities between $20\text{--}40$ kms^{-1} following the peak of emission, and reaches an altitude of $30,000\text{--}40,000$ km. There are noticeable irregularities in the height measurements, which they suggest are due to transient heating events or confinement of plasma. Feldman and Seely (1995), have made use of Skylab and Yokoh observations and concluded that there is no relationship between the hot and cool loops and the cool loops do not necessarily lie below the hot loops, hence the chosen model should not depend on the appearance of cool loops below hot loops. Feldman et al., 1995 analysed two LDEs in detail concentrating on their morphology and plasma parameters. The plasma pressure is found to be greater at the bright region near the looptop than in the loop legs. Despite the difference in pressure between the two regions, the bright looptop region stays confined for a number of hours. This observation is in contradiction with numerical simulations of the chromospheric evaporation model leading us to the conclusion that the hot material would cool by conduction and radiation on the order of minutes. They suggest that the bright region is not a single heated plasma region, but rather is a large number of small bright regions continually regenerated by some, as yet unknown, process. They do not rule out the standard reconnection models, but expect changes in the magnetic configuration in which energy release should occur.

The maximum X-ray energy which has been observed in post-flare loops is $8\text{--}11.5$ keV from HXIS on SMM. One aspect which has not been analysed in detail is how the higher temperature component rises with time. Does it rise with the same velocity as the soft X-ray (SXR) source? A detailed analysis of the previous hard X-ray (HXR) sources of compact flares showed indications of magnetic reconnection (e.g. Masuda et al, 1994). This appears in the form of a hard X-ray source lying above the soft X-ray loop, in addition to two hard X-ray sources at the footpoints. The looptop source is believed to be either the reconnection site or the site where the reconnection outflow impinges on the higher density soft X-ray loop. The centroid position of

this source is higher than the soft X-ray loop by $\approx 10''$ and is located at higher altitudes for images with higher energy. The looptop source exists temporally on the order of a few minutes and has a size of $\approx 5\text{--}10''$. There are many difficulties involved with carrying out a similar analysis for LDEs to that carried out for the compact flares discussed by Masuda. The problems are discussed briefly by Sato et al. (1996), where they have analysed an LDE using a new technique which enables HXT image synthesis of larger HXR sources, and the construction of images in the decay phase of flares. Sato (1997) has accurately estimated the instrumental response function and improved the HXT image synthesis procedure. The source sizes of the events that were analysed are more than 1 arcmin. He finds that the brightest core of the HXR source is sometimes co-spatial with and sometimes above the soft X-ray looptop region. The shape of the HXR source is indicative of a high temperature cusp region tracing an arcade of loops.

The purpose of this work is to analyse LDEs which have good coverage in HXR, SXR and $H\alpha$. It was also necessary to have HXR imaging capability. This was the most difficult aspect since it is vital to have good quality HXR images beyond the peak of the flare. We study two LDEs - one on the 28 June 1992, which is one of many large flares in active region NOAA 7205 (van Driel-Gesztelyi et al. 1997b), and the 2 November 1992 event, which was one of the flares analysed by Feldman et al. (1995). For these events we have determined the altitudes of not only the $H\alpha$ and soft X-ray loops, but also the heights of the hot sources determined on the basis of HXT observations using the technique developed by Sato (1997). This provides an insight into the physical process which maintains emission for more than eight hours.

2. Instruments

2.1. Yokoh

For this analysis we make use of two of the instruments on board Yokoh – the grazing incidence soft X-ray telescope (SXT) and the hard X-ray telescope (HXT). SXT has been described in detail by Tsuneta et al. (1991). It is sensitive to X-rays in the energy range $0.25\text{--}4.0$ keV. Our data were obtained in full resolution mode (pixel size = $2.46''$) with 64×64 pixel field-of-view in FLARE mode.

The Hard X-ray Telescope (HXT), described by Kosugi et al. (1991), is a Fourier synthesis imager of 64 elements. It employs 4 channels covering the range $15\text{--}100$ keV with a time resolution of 0.5 seconds. The images were synthesised using the Maximum Entropy Method (MEM) with the new instrument response function and revised MEM algorithm including systematic variations as described by Sato (1997).

2.2. Ground-based

For the 28 June 1992 event we used Wrocław data obtained in $H\alpha$ by the Small Coronagraph (pass band 3 \AA), the Large Coronagraph (pass bands 0.5 \AA and 3 \AA) and the Solar Horizontal

Table 1. Times of the flares and of the observations obtained by GOES, SXT and ground-based observations (GBO).

	28 June 92	2 Nov 92
Position	N11W	S26W
Flare time	04:45-13:00	02:45-18:00
Flare max	05:05	03:04
GOES class	X1	X9
HXT obs	03:51-04:50	02:59-03:25
	05:28-05:56	04:37-05:38
SXT obs	03:51-04:50	03:04-03:35
	05:28-05:56	04:41-05:38
GBO obs	04:02-09:19 ^a	04:22-05:24 ^d
	05:26-14:59 ^b	03:37-06:43 ^e
	07:34-13:27 ^c	

a– Wrocław Large Coronagraph (band path 0.5 Å), b– Bialkov horizontal telescope (band path 0.5 Å), Wrocław Solar Horizontal Telescope (pass band 0.5 Å) c– Wrocław Small Coronagraph (pass band 3 Å), d– Hiraiso, e– Mitaka

Telescope (pass band 0.5 Å). The event of 2 November 1992 was continuously observed in many observatories in Japan (Hiraiso, Mitaka, Hida, Norikura). We used data from the Solar Flare Telescope in Mitaka which observed in H α , and the H α Solar Telescope in Hiraiso (Akioka, 1996).

3. Observations

We have selected two LDEs which are well observed in H α hydrogen line as well as soft and hard X-rays. The times and sources of the data analysed are depicted in Table 1. Both events are limb flares and large systems of post-flare loops developed within a few hours of the flare initialisation.

Fig. 1 illustrates the GOES (Geostationary Orbiting Environmental Satellites) data for both events. Both flares reach extremely high GOES class - the 2 November event being one of the largest flares observed by Yohkoh, saturating the GOES data.

Both flares have similar profiles in that the impulsive phase is short and the decay phase lasts many hours. This is typical of the behaviour of LDEs. Figs. 2 and 3 show the HXR light curves for both events. Typical hard X-ray bursts last on the order of a few minutes. In these two examples the time profiles of the hard X-rays are smooth and survive approximately an hour in both cases in all HXT channels. Images could be obtained only in the L channel (15–24 keV). In the following sections we discuss the details of both flares separately, including any previous relevant work.

3.1. 28 June 1992

Many large flares occurred in active region NOAA 7205, and have subsequently been studied in detail by van Driel-Gesztelyi et al. (1997b). The latter paper describes how shear and emerging flux can be responsible for such large events in a δ spot region. One of these events (25/26 June 1992) has already been intensively studied by Schmieder et al. (1995, 1996), van Driel-

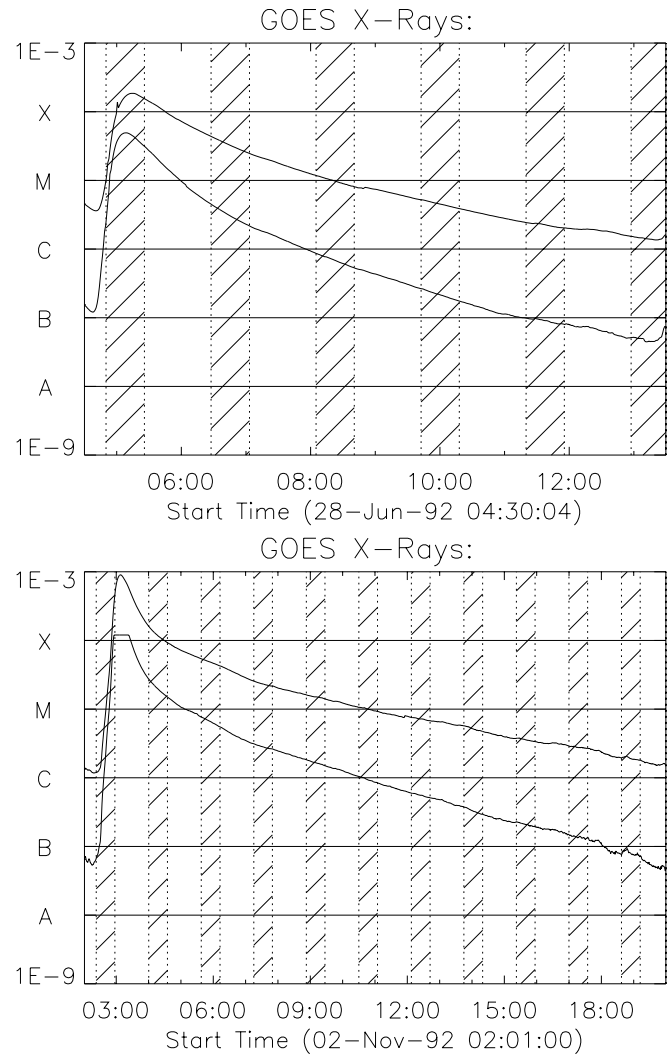


Fig. 1. The top panel shows the X-ray emission as recorded by the GOES 1–8 Å channel (top curve) and the 0.5–4.0 Å channel (lower curve) for the LDE on the 28 June 1992. The lower panel shows the same plot for the 2 November 1992 LDE. The shaded areas illustrate the times when the Yohkoh spacecraft is in night mode.

Gesztelyi et al. (1997a), Malherbe et al. (1997) and Moore et al. (1997). By the time the LDE on the 28 June 1992 occurred, AR 7205 was $\approx 4^\circ$ behind the limb and only post-flare looptops were visible. The development of the loops was followed for nearly 11 hrs with the Wrocław solar instrumentation.

Yohkoh/SXT was observing for only a few minutes during the impulsive phase of the flare, and then after 10:17 UT, in the decay phase, observations are again available (see Fig. 1). SXT observed using 2 filters (Al1 and Be). The data have been reduced using the standard Yohkoh software. The SXT and H α images have been carefully co-aligned - the results are shown in Figs. 4 and 5.

Using the new MEM image synthesis technique we obtained HXR images from the L channel. These are shown along with the SXR images in Fig. 6. Unfortunately the Yohkoh SXT was pointing at a different active region prior to 05:34 UT. The HXR

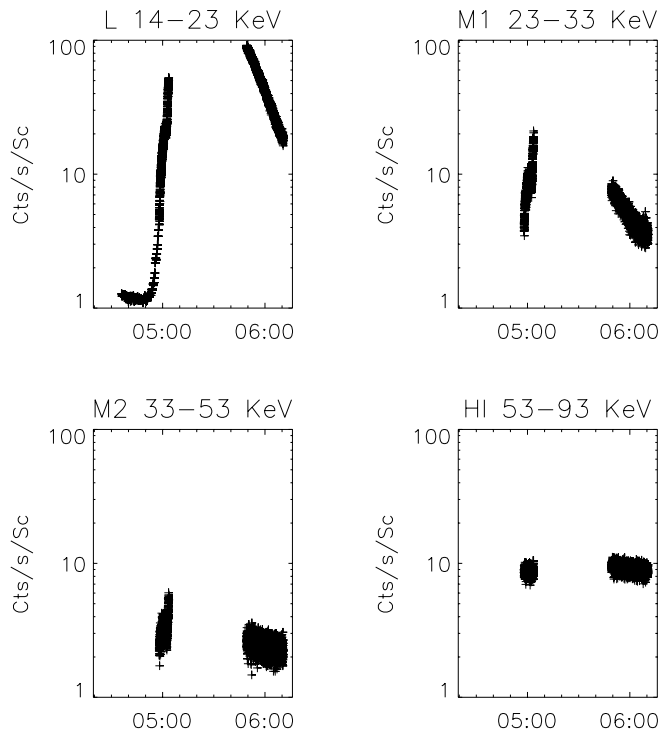


Fig. 2. The light curves from the HXT in all 4 channels for the LDE on the 28 June 92. There is significant HXR emission in all channels lasting for more than one hour.

images show several sources. The trend is for the source to lie slightly above the SXR structures with part of the HXR structures lying on top of the SXR structures. This is consistent with the results of Sato (1997).

3.2. 2 November 1992

The flare occurred in active region NOAA 7321 which is already behind the limb by $\approx 3^\circ$ at the start of the event ($\approx 02:30$ UT). We have also used the ground-based observations made in Mitaka and Hiraiso. We have observations for a few hours after the impulsive phase of the flare showing the development of post-flare loop systems. Some preliminary analyses have been published (Ichimoto et al. 1994, Harra-Murnion et al. 1997, Feldman et al. 1995).

Feldman et al. (1995) concentrated on the morphology and plasma parameters of this flare. They discuss the region at the top of the loop which is initially circular ($\approx 20,000$ km), and lasts for several hours, finally becoming elongated. They argue that the confinement of this bright looptop for such a long period of time is in disagreement with current models, particularly numerical simulations of chromospheric evaporation.

Ichimoto et al. (1994) have analysed this flare using X-ray, $H\alpha$ and continuum data. They looked at the geometrical relationship between the X-ray source and the $H\alpha$ source and calculated the energy balance. They noted that the X-ray images show less distinct loop structures than the $H\alpha$ and commented that this must be a physical effect and not due to lack of resolu-

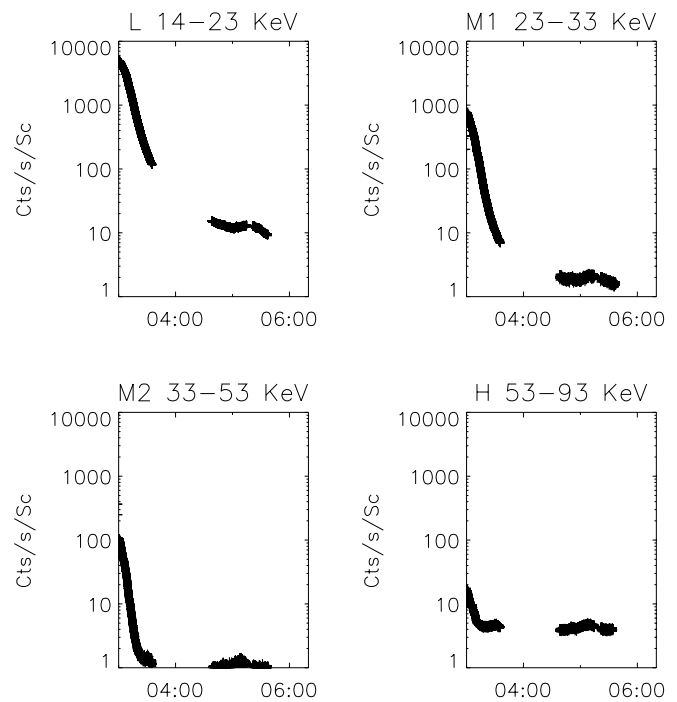


Fig. 3. The light curves from the HXT in all 4 channels for the LDE on the 2 November 1992. There is significant HXR emission in all channels lasting for several hours.

tion. Calculating the gas and magnetic pressures they find that the gas pressure exceeds the magnetic pressure, suggesting that the magnetic field is not strong enough to confine the hot plasma as rigidly as is commonly assumed in theories. However, they find that the geometrical and temporal relationship between the hot and cool plasma are consistent with the standard scenario of successive reconnection towards the higher corona.

Co-aligned $H\alpha$ and SXR images are shown in Figs. 7 and 8 at 04:49 and 05:37 UT respectively. We see clearly that the cool loops lie tangentially below the soft X ray loops. As for the 28 June event, we also produced HXR images in the L channel. These are shown in Fig. 9. The bulk of the HXR source lies above the SXR loop structures. The source appears to grow larger as time progresses. This is also apparent in Fig. 9 where more sources appear with time. The source is larger than the compact flare sources discovered by Masuda et al. (1994). In the case of these LDEs it can be on the order of $20 - 45''$, compared to the $10''$ in the compact flares.

4. Altitude measurement

For both events, the footpoints are hidden behind the limb. We measure the altitude from the limb to the top of the loop. We did not apply corrections for rotation since the locations of the footpoints are uncertain. So the altitude and velocity measurements will be slightly affected but this is however insignificant relative to the size of the error bars (rotation produces an error of $\approx 1,000$ km for the altitude). In the case of the SXR images where the looptop is not distinct we chose the maximum intensity of

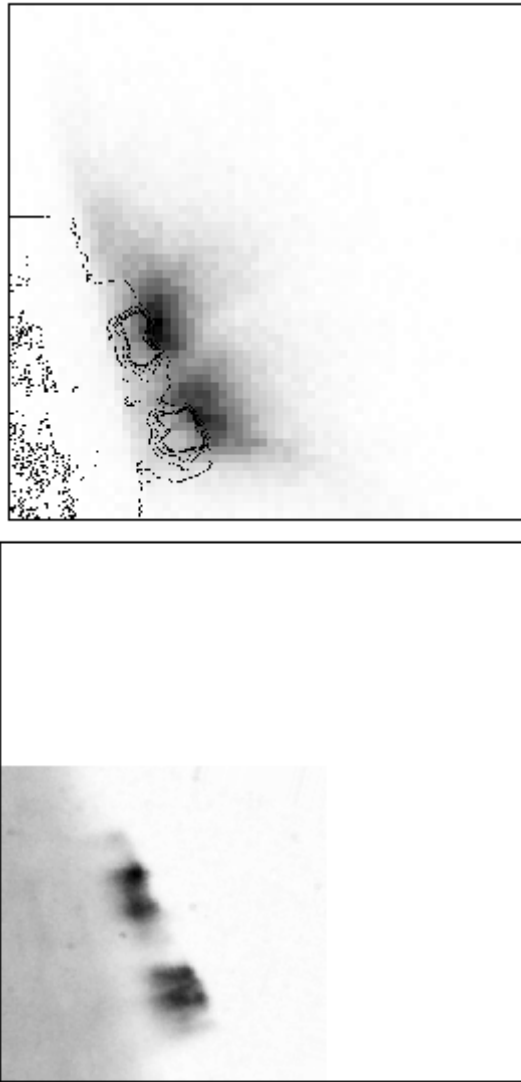


Fig. 4. The top panel shows the SXT image in the thin Al filter at 05:40 UT on the 28 June 92 with the $H\alpha$ image overlaid as contours. The image size is $\approx 160 \times 160$ arcsecs. The W limb is visible. The lower panel shows the $H\alpha$ image. It is clear that the $H\alpha$ loops lie below the SXR loops.

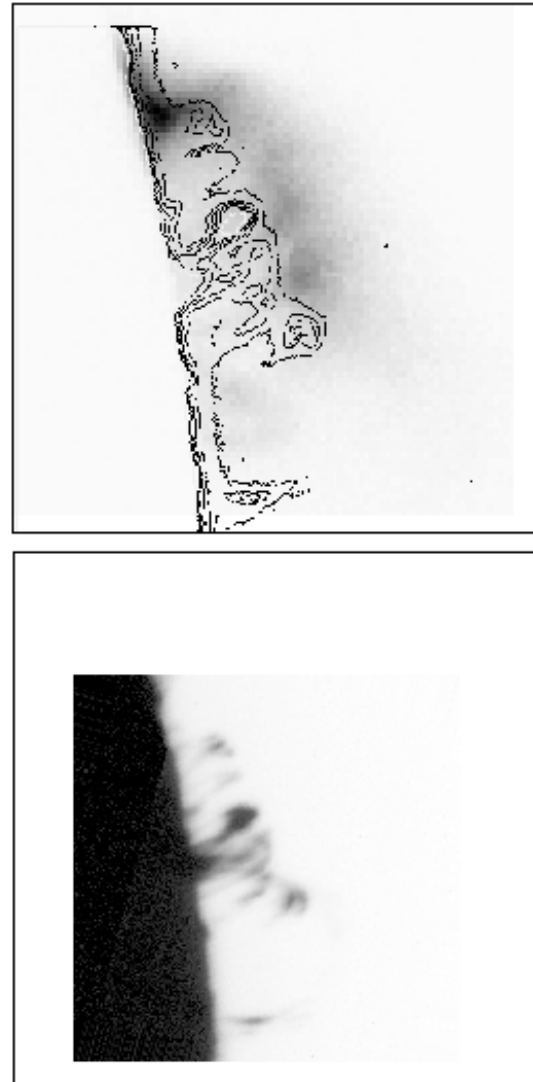


Fig. 5. The top panel shows the SXT image of the 28 June flare in the thin Al filter at 11:11 UT with $H\alpha$ contours. The image size is $\approx 160 \times 160$ arcsecs. It is clear that within a few hours both loops systems have risen significantly. The lower panel shows the $H\alpha$ image at 11:11 UT.

the looptop. This area is generally confined to a circular bright region as discussed in Feldman et al.(1995). We measure only one section of each loop system - this is illustrated by arrows in Figs. 5 and 7. To measure the HXR sources we concentrate on the region above the SXR loop of interest. Since the statistics of the signals of the images are relatively low we measured the peak centroid region and the area around this region which was within 75 % of the peak. From these measurements we obtained the error bars as shown in Figs. 10 and 11. The error bars for both the SXR and $H\alpha$ loop altitudes are assumed to be 2 pixels.

4.1. 28 June 1992

The time-altitude diagram (Fig. 10) shows that the height difference between the $H\alpha$ and X-ray loops is increasing with time.

We measure only one loop as indicated by the arrow in Fig. 6. It is not possible to follow the HXR image for a long period of time due to the poor count statistics later in the event. The HXR source does appear to rise with time in this case but slower than the SXR loops.

At the beginning (just before 06:00 UT) the height difference is very small between the SXR and $H\alpha$ loops. Some hours later on, at around 11:00 UT, the higher stretched loops displayed a larger height difference between the cool and hot loops. Therefore the time difference to cool from X-ray to $H\alpha$ loops is longer later in the event. We are only able to measure the HXR source for 30 minutes at the beginning of the rise of the post-flare loop system. Initially both the SXR and $H\alpha$ loops rise at speeds of 3.2 and 2.2 kms^{-1} respectively. At the end of our observations the velocity has fallen to 0.3 and 0.1 kms^{-1} respectively. The

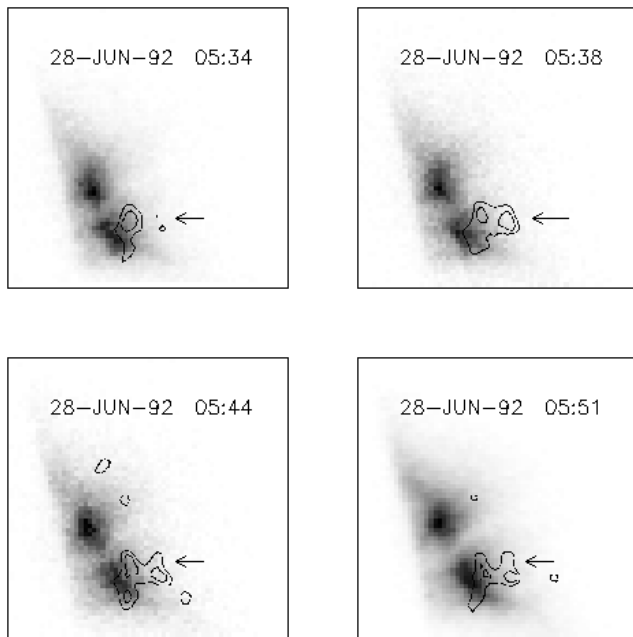


Fig. 6. This illustrates a raster of SXR images, with the L channel HXR images overlaid as contours for the flare of 28 June 1992. The 75 % and 50 % contour levels are shown. Arrows indicate the loop studied. The image size is $\approx 160 \times 160$ arcsecs.

average velocity of the HXR source is $\approx 2 \text{ kms}^{-1}$. The error bars on the HXR source height measurement are large due to the large spatial extent of the source. We are only able to produce synthesised HXR images for the L channel (14–23 keV), which is not strictly non-thermal, but will have a thermal contribution. We measured the temperature using the ratios from the L (14–23keV)/M1(23–33 keV), and obtained a value of between 19 – 26 MK. The bright SXR looptop region during the same time period had a temperature of 8–10 MK using the ratio of the Be and thick Al filters. The SXT filter ratio technique is described in detail by Hara (1992).

4.2. 2 November 1992

Fig. 11 shows the altitude measurements for the $\text{H}\alpha$ (Hiraiso and Mitaka) the soft X-ray (SXR), and Hard X-ray (HXR) structures. The structure that was measured is indicated by an arrow in Fig. 9. In this case the SXR and $\text{H}\alpha$ rise with time with speeds of 5.4 – 1.1 and 4.8 – 1.1 kms^{-1} respectively. The HXR source rises with a speed of approximately 3 kms^{-1} . It is obvious from the figure that the SXR and HXR emission move further apart as time progresses. The temperature of the SXR and HXR sources were measured in the same way as for the 28 June event; the values range from 8.5–10.5 MK and from 17–27 MK respectively.

5. Cooling times

To determine the cooling times we measure the temperature and emission measure from SXT using the filter ratio technique (Be

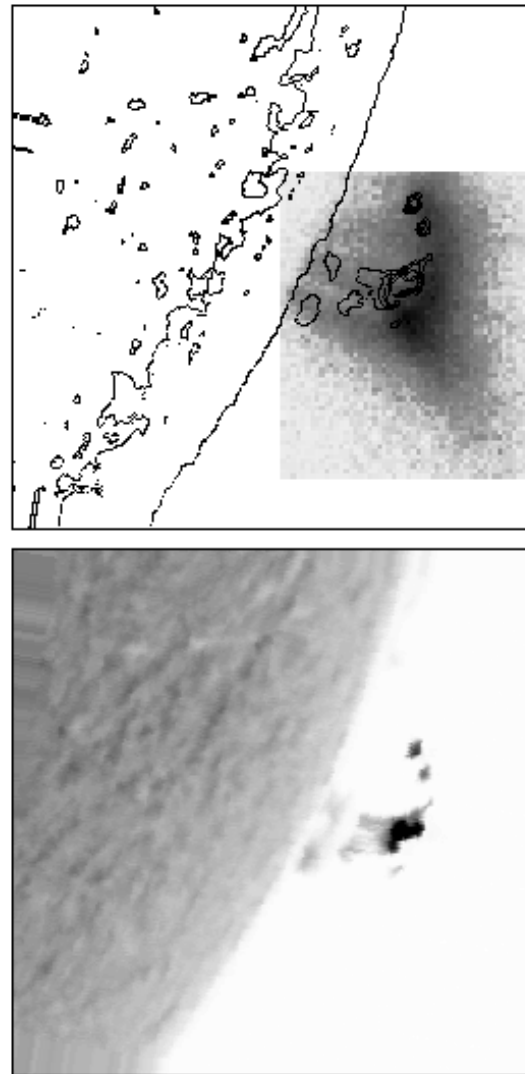


Fig. 7. The top panel shows the SXT image of the 2 Nov flare in the Be filter at 04:49 UT with the $\text{H}\alpha$ image overlaid in contours. The W limb is visible. The lower panel shows the $\text{H}\alpha$ image. It is clear that the $\text{H}\alpha$ loops lie below the SXR loops. The image size is $\approx 266 \times 266$ arcsecs.

and thick Al). Our measurements concentrate on the tops of the loops.

The critical parameter in determining the cooling time is the density. The area can be measured from the images, but an estimate for the depth has to be made. We made the same assumptions for both flares. We assumed that the area is all pixels greater than $0.5 \times \text{Intensity}_{max}$. Since we cannot measure the depth directly we assume a value of $\sqrt{\text{area}}$. This will give an upper limit to the depth and hence a lower limit to the density. As discussed in Cargill et al. 1995 the values of the cooling times are sensitive to the density. Table 2 illustrates the affect of the depth assumptions on the cooling time for the 2 November flare at 03:50.

Cargill et al. (1995) give an analytic solution to the problem of the cooling of hot loops which assumes that during the evo-

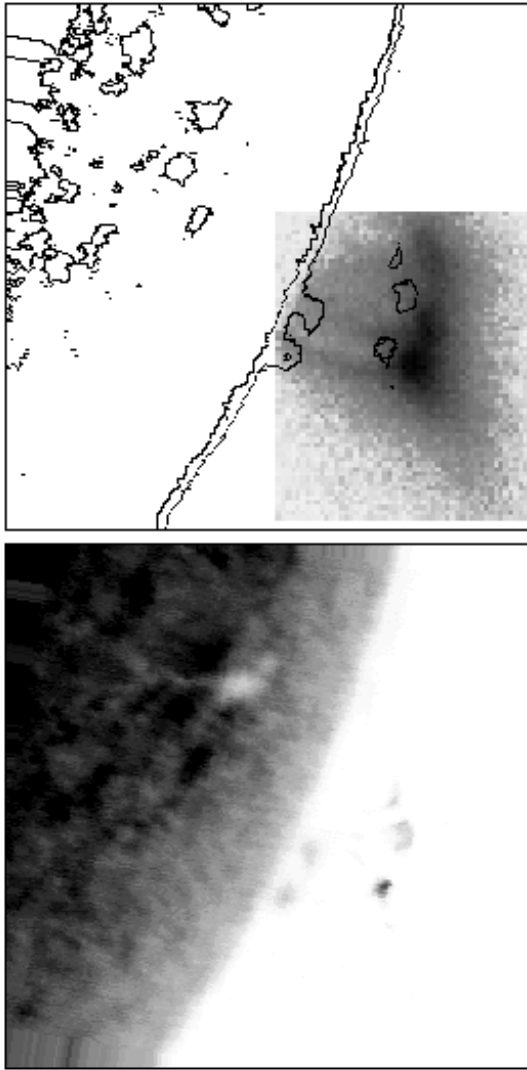


Fig. 8. The top panel shows the SXT image in the Be filter of the 2 Nov flare at 05:37 UT with the $H\alpha$ image overlaid in contours. The lower panel shows the $H\alpha$ image. It is clear that within a few hours both loop systems have risen significantly. The image size is $\approx 266 \times 266$ arcsecs.

Table 2. The affect of varying the depth on the cooling time on the 2 November flare at 03:50 U.T. using the method of Cargill et al. 1995.

Depth (km)	10,000	20,000	30,000	40,000	50,000
Volume (10^{28} cm^3)	2.2	4.4	6.7	8.9	11
Density (10^{10} cm^{-3})	7.5	5.3	4.3	3.7	3.3
T_{cool} (mins)	33	37	38	40	41

lution of the flare, conductive cooling initially dominates with radiative cooling taking over later on. The observed cooling time was deduced from the altitude plots of X-ray and $H\alpha$ loops. At any given altitude the horizontal distance (along the time axis) between the X-ray and $H\alpha$ loop gives the time necessary for a given hot loop to cool down and appear in $H\alpha$. A range of values is given for the observed cooling time to account for the errors in measuring the altitudes. Table 3 illustrates the values

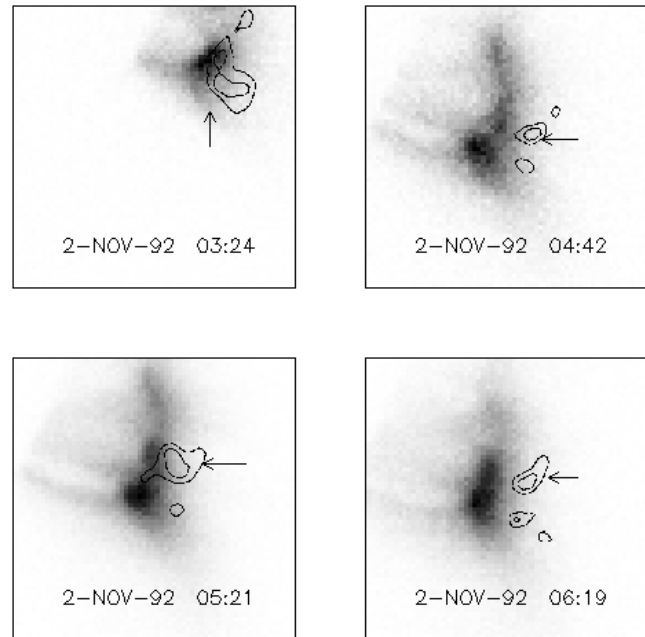


Fig. 9. This illustrates a raster of SXR images, with the L channel HXR images overlaid as contours for the flare of 2-Nov-92. The 75 % and 50 % contour levels are shown. An arrow shows the area of the loop system which we concentrate on. The image size is $\approx 160 \times 160$ arcsecs.

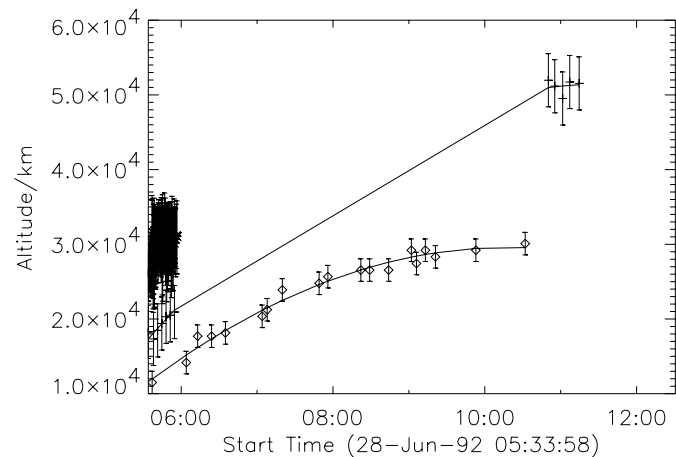


Fig. 10. The altitude of the SXR (crosses), $H\alpha$ (open diamonds) and HXR L channel (asterisks) for the 28 June 1992 event. Since the HXR source is not symmetrical and extended, the error bars were determined by taking a range within 75% of the peak contour. The errors in the SXR and $H\alpha$ are assumed to be 2 pixels.

determined at 2 times for the 2 November flare. The calculated cooling times are within the range of the observed cooling times for both times. A similar analysis was carried out on the 28 June 1992 LDE (Table 4).

Previous observations have found that there is good agreement between the theory and observed cooling times early in the flare decay, but that the discrepancy tends to increase late in the decay phase (e.g. van Driel-Gesztelyi et al. 1997a, Wiik et al.

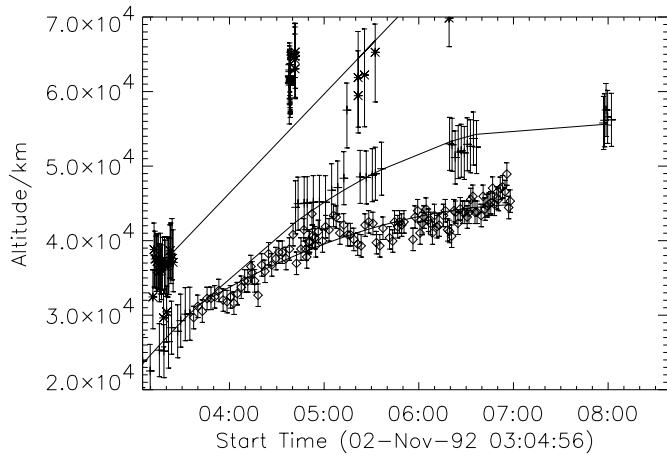


Fig. 11. The altitude of the SXR (crosses), $H\alpha$ (open diamonds) and HXR L channel (asterisks) for the 2-Nov-92 event. Since the HXR source is not symmetrical and extended, the error bars were determined by taking a range within 75% of the peak contour. The errors in the SXR and $H\alpha$ are assumed to be 2 pixels.

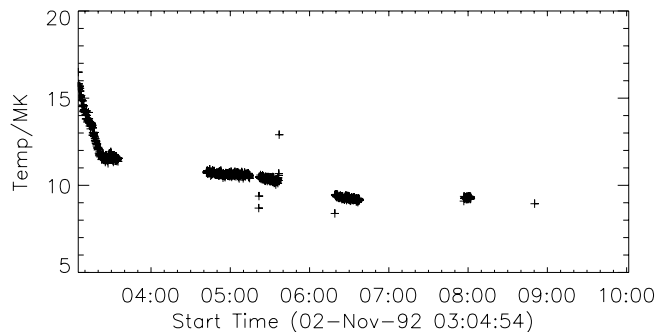
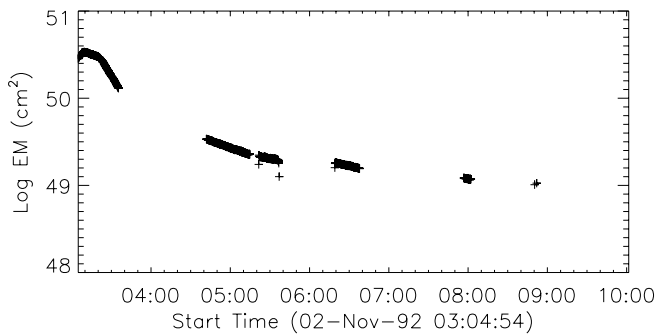


Fig. 12. The Emission Measure (EM) and Temperature as derived from the filter ratio technique using the Be and thick Al filters for the 2 November flare

1997). In 28 June case, later in the flare, the calculated values are less than the observed values. There are several explanations for this difference. There are uncertainties in the calculation of the electron density and also the methods of calculation. Furthermore, field line shrinkage is one possibility, as discussed in Švestka et al. (1987b) and additional heating of the loops during the cooling process would extend their cooling time.

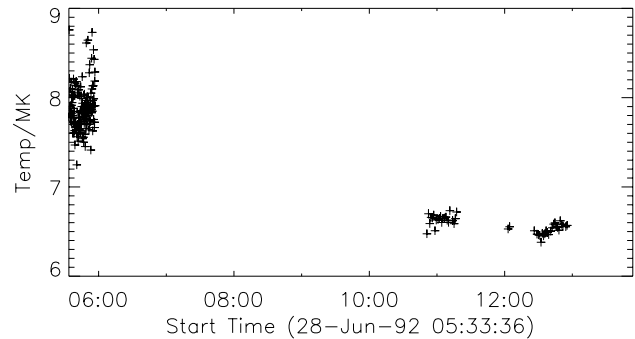
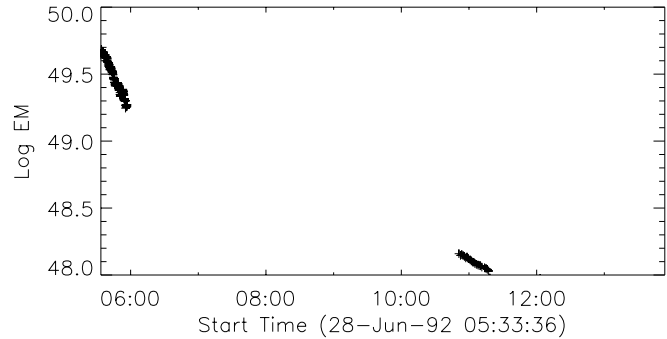


Fig. 13. The Emission Measure (EM) and Temperature as derived from the filter ratio technique using the Be and thick Al filters for the 2 November flare

Table 3. Cooling times calculated and observed for the 2 November event using an initial temperature of 15 MK.

Time UT	Log (EM)	Ne cm^{-3}	Semi length (km)	Obs T_c	Calc T_c
03:35	50.1	3.4×10^{10}	3.1×10^4	0 → 42	41
05:36	49.3	1×10^{10}	5.2×10^4	25 → >110	80

Table 4. Cooling times calculated and observed for the 28 June event using an initial temperature of 8 MK.

Time UT	Log (EM)	Ne cm^{-3}	Semi length (km)	Obs T_c min	Calc T_c min
05:33	49.6	2.4×10^{10}	2×10^4	25 → 90	32
10:51	48.1	2.2×10^9	5.5×10^4	>100	73

6. Discussion and conclusions

In this paper we have analysed two LDEs, not only in $H\alpha$ and in soft X rays as the previous studies have done (Schmieder et al. (1995, 1996), van Driel-Gesztelyi et al. (1997a)) but also in hard X-rays.

From the two events that we studied in detail we observe that the cool and hot loops are connected in some way. They have similar morphology with the X-ray loops lying above the cool $H\alpha$ loops. Some loops which appear in $H\alpha$ do not have a corresponding X-ray loop visible in SXT images. This occurs because they are not hot enough or the emission measure is too small to be seen above the SXT intensity threshold. We

do not however see the jumps in altitude which Feldman and Seely (1995) predict from the reconnection model. In fact the reconnection process can be smooth and continuous.

We found the calculated flare cooling times to be consistent with those deduced from observations for the first few hours into the decay phase, but the calculated cooling times were longer than the observed late in the flare decay phase. This was found for the cooling times calculated by Cargill et al. (1995) which tend to be longer than the cooling times determined by Švestka (1987a). The results indicate that an additional source of heating, for example, is required late in the decay phase, or an improvement in the method of cooling time calculations.

Various observational evidence support the hypothesis of magnetic reconnection as the main energy source. One of the observations supporting this is the evidence of HXR sources lying above the SXR loops (Masuda et al. 1994). These were observed in compact flares only. Due to the work carried out by Sato et al. (1997) in recalibrating the HXT instrument, we are now able to study the HXR sources of LDEs. For the two cases we have studied we find that the L channel HXR source lies above and slightly overlapping the SXR loops. The L channel of HXT has two components – one thermal and one non-thermal. However this source is indicative of a higher temperature region. We have as yet been unable to carry out a similar analysis for the higher energy channels. The extended HXR source is maintained for a much longer time period than the compact sources in impulsive flares. The compact sources exist for several minutes while the LDE HXR sources last many tens of minutes. The source size of the LDE HXR source is larger than impulsive flare HXR sources by a factor of approximately 5.

It is also interesting to note that the HXR sources exist close to the SXR loop. As time progresses the HXR source and the SXR loop become further apart. Since the HXR source is extended it is not possible to determine accurately the speed of the change involved. From the Kopp and Pneumann picture it may be expected that the SXR loop and the HXR source ('reconnection point') would rise simultaneously. Another possibility is that we are observing a section of a hotter loop structure. If this is the case then the differences in the relative positions of the structures could be due to field line shrinkage as suggested by Forbes & Acton (1996). Recent modelling work by Karpen, Antiochos & DeVore (1996) constructed a realistic situation in which the initial multipolar field is asymmetric. A result of this situation is ongoing reconnection that occurs sporadically along the current sheet. The evolution is complex compared to the Petschek model. Frequently two reconnection points can occur somewhere along the sheet resulting in the formation of a magnetic island. The end result of this random reconnection is that the post-reconnection flux is filled with current sheets. The main difference between this simulation and previous ones is that the heating would be due to the dissipation of many intense current sheets, which means that the heating process is long-lived. The randomness of the reconnection also fits in with our observations since the HXR source is extended and several sources can exist simultaneously. As more current sheets are formed the size of the region being heated increases. Also if the

reconnection process is sporadic it follows that the velocity of the rising reconnection site need not necessarily be the same as the SXR loops and the $H\alpha$ loops.

Shibata (1997) has discussed the possibility of a plasmoid induced reconnection model in which plasmoid ejection is the main trigger for reconnection. He discusses the possible differences between HXR looptop sources observed in impulsive flares and those observed in LDEs. He expects the HXR source in impulsive flares to lie high above the soft X-ray loop due to the larger inflow velocity producing faster reconnection. Subsequently the MHD fast shock is produced above the SXR loop. However in the case where the inflow velocity is slow the reconnection is slow and hence the fast shock is created at the SXR loop. In our events we observe the HXR source to overlap slightly with the SXR loop but still lying above it, which is consistent with the predictions of Shibata. However there is no discussion in the work on how the HXR source would be expected to rise.

The idea of turbulence to maintain the high temperatures reached during the impulsive phase of flares was discussed by Jakimiec (1990). The regions of energy release in a high density, turbulent volume (post-impulsive phase), can occupy most of the hot plasma volume, and supply sufficient energy release to explain the plasma heating and maintenance at ≈ 20 MK. Tomczak (1997) observed the impulsive phase of an arcade event. He finds that there was more than one location of energy release at the looptops. He relates this to Jakimiec's model in which the energy release occurs in turbulent regions - the electrons are accelerated in this region to energies > 20 keV. We observe the same behaviour for the looptop, with several HXR sources appearing along the top of the arcade well into the gradual phase.

In summary, our observations illustrate the complexity of the behaviour of post-flare loop systems. It is found that the separation between the HXR source and the SXR loop tends to increase with time. A number of present models are consistent with our observations. To narrow the process further we intend to extend this work to the UV wavelength region using data from the SOHO mission. Also the upcoming High Energy Solar Spectroscopic Imager (HESSI) will have a high sensitivity and large dynamic range which will be capable of covering from the peak of the flares well into the decay phase.

Acknowledgements. LKHM would like to thank PPARC for post-doctoral funding. LVDG acknowledges the Hungarian research grant T17325 OTKA. BR and PR acknowledge the Polish Committee for Scientific Research grant 2.P03D.025.09. This paper could be achieved because of the Royal Society collaboration program. We would also like to thank Dr. Pascal Démoulin for valuable discussions, Dr. Ludwig Klein for information on radio burst locations observed by the Nançay radioheliograph and Dr Hiroki Kurokawa for discussions on the observations of the 2 November flare. Finally our thanks goes to Dr. P. Cargill for his interest and discussions on the problem of loop cooling.

References

- Akioka M., 1996, *J. Geomag. Geoelectr.* 48, 5
- Bray R.J., Cram L.E., Durrant C.J. and Loughhead R.E. 1991, *Plasma Loops in the Solar Corona*, Cambridge Astrophysics Series

- Bruzek A. 1964, *ApJ* 140, 2
- Cargill P.J. and Priest E.R., 1983, *ApJ* 266, 383
- Cargill P.J., Mariska J.T., and Antiochos S., 1995, *ApJ* 439, 1034
- Feldman U. and Seely J.F. 1995, *ApJ* 450, 902
- Feldman U., Seely J.F., Doschek G.A., Brown C.M., Phillips K.J.H., and Lang J. 1995, *ApJ* 446, 860
- Forbes T.G. and Malherbe J.M. 1986, *ApJ* 302, L67
- Forbes T.G. and Acton L.W. 1996, *ApJ* 459, 330
- Hara H., 1992, Master thesis, Dept. of Astronomy, University of Tokyo
- Harra-Murnion L.K., Plunkett S.P., Helsdon S.F., Phillips K.J.H., van Driel-Gesztelyi L., Schmieder B., Rompolt B., Akioka M., 1997, *Adv. Space Sci.*, Vol. 20, No. 12, 2333
- Ichimoto K., Sakurai T. et al. 1994, 2nd Japan-China meeting, Sagami-hara, eds Sakurai T., Hitayama T., Ai G., 94, 151
- Jakimiec J. 1990, *Adv. Space. Res.*, Vol. 10 No. 9, 109
- Karpen J.T., Antiochos S.K. and DeVore C.R. 1996, *ApJ* 460, L73
- Kopp R.A. and Pneumann G.W., 1976, *Solar Phys.* 50, 85
- Kosugi T. et al. 1991, *Solar Phys.* 136, 17
- MacCombie W.J., and Rust D.M. 1979, *Solar Phys.* 61, 69
- Malherbe J.M., Tarbell T., Wiik J.E., Schmieder B., Franck Z., Shine R.A. and van Driel-Gesztelyi L., 1997, *ApJ* 482, 535
- Masuda S., Kosugi T., Hara H., Tsuneta S., Ogawara Y., 1994, *Nature* 371, 495
- Moore R. et al. 1980, in *Solar Flares - A monograph from Skylab Solar Workshop II*, Ed P. Sturrock, Colorado Associated University Press
- Moore R.L., Schmieder B., Hathaway D.H., Tarbell T.D., 1997, *Solar Phys* 176, 153
- Pneuman G.W., 1981, In *Solar flare MHD* ed E.R. Priest P379-428, New York Gordon and Breach
- Sakao T. 1994, PhD thesis, University of Tokyo
- Sato J. 1997, PhD thesis, Graduate University of Advanced Science, Tokyo
- Sato J., Kosugi T., and Sakao T. 1996, *Magnetodynamic Phenomena in the Solar Atmosphere*, ed. Y. Uchida, T. Kosugi and H.S. Hudson, Kluwer Academic Press, p545
- Schmieder B., Heinzel P., Wiik J.E., Lemen J.R. and Hiei E. 1995, *Solar Phys* 156, 337
- Schmieder B., Heinzel P., van Driel-Gesztelyi L., Lemen J.R. 1996, *Solar Phys* 165, 303
- Seely J.F. and Feldman U. 1984, *ApJ* 280, L59
- Shibata K. 1997, *Proc. 5th SOHO workshop*, ESA pub SP-404, 103
- Švestka Z.F., 1987a, *Solar Phys (Letters)*, 108, 411.
- Švestka Z.F., Fontenla J.M., Machado M., Martin S.F., Neidig D.F., and Poletto G., 1987b, *Solar Phys* 108, 237
- Švestka Z.F., 1996, *Solar Phys* 169, 403
- Tomczak M. 1997, *A&A* 317, 223
- Tsuneta S. 1991, *Solar Phys* 136, 37
- Tsuneta S. et al. 1992, *PASJ* 44, L63
- Tsuneta S. 1996, *ApJ* 456, 840
- van Driel-Gesztelyi L., Wiik J.E., Schmieder B., Tarbell T., Kitai R., Funakoshi Y., Anwar B. 1997a, *Solar Phys*, 174, 151
- van Driel-Gesztelyi L., Csepura G., Schmieder B., Malherbe J.M., and Metcalf T., 1997b, *Solar Phys* 172, 151
- Wiik J.E., van Driel-Gesztelyi L., Schmieder B., Heinzel P., 1997, *Adv. Space Res.*, Vol. No. 20, 2345